Archives of Biochemistry and Biophysics 509 (2011) 9–15

Contents lists available at ScienceDirect

Archives of Biochemistry and Biophysics

journal homepage: www.elsevier.com/locate/yabbi

Heterologous expression and characterization of the sterol 14α-demethylase CYP51F1 from *Candida albicans*

Hyoung-Goo Park [a], Im-Soon Lee [a], Young-Jin Chun [b], Chul-Ho Yun [c], Jonathan B. Johnston [d], Paul R. Ortiz de Montellano [d], Donghak Kim [a,*]

[a] Department of Biological Sciences, Konkuk University, Seoul 143-701, Republic of Korea
[b] College of Pharmacy, Chung-Ang University, Seoul 156-756, Republic of Korea
[c] School of Biological Sciences and Technology, Chonnam National University, Gwangju 500-757, Republic of Korea
[d] Department of Pharmaceutical Chemistry, University of California, San Francisco, CA 94158, USA

ARTICLE INFO

Article history:
Received 18 November 2010
and in revised form 31 January 2011
Available online 17 February 2011

Keywords:
P450
CYP51
Lanosterol
Azole
Candida albicans

ABSTRACT

Lanosterol 14α-demethylase (CYP51F1) from *Candida albicans* is known to be an essential enzyme in fungal sterol biosynthesis. Wild-type CYP51F1 and several of its mutants were heterologously expressed in *Escherichia coli*, purified, and characterized. It exhibited a typical reduced CO-difference spectrum with a maximum at 446 nm. Reconstitution of CYP51F1 with NADPH-P450 reductase gave a system that successfully converted lanosterol to its demethylated product. Titration of the purified enzyme with lanosterol produced a typical type I spectral change with K_d = 6.7 μM. The azole antifungal agents econazole, fluconazole, ketoconazole, and itraconazole bound tightly to CYP51F1 with K_d values between 0.06 and 0.42 μM. The CYP51F1 mutations F105L, D116E, Y132H, and R467K frequently identified in clinical isolates were examined to determine their effect on azole drug binding affinity. The azole K_d values of the purified F105L, D116E, and R467K mutants were little altered. A homology model of *C. albicans* CYP51F1 suggested that Tyr132 in the BC loop is located close to the heme in the active site, providing a rationale for the modified heme environment caused by the Y132H substitution. Taken together, functional expression and characterization of CYP51F1 provide a starting basis for the design of agents effective against *C. albicans* infections.

© 2011 Elsevier Inc. All rights reserved.

Introduction

Cytochrome P450s (P450s, CYPs)[1] are heme-thiolate-containing enzymes that catalyze reactions involving both endogenous and exogenous substrates [1,2]. These enzymes are found throughout nature and in microorganisms play important roles, particularly in the biosynthesis of antibiotics and other biologically active molecules [3]. Genomic analysis of *Candida albicans* suggests that it contains 10 putative P450 enzymes, including CYP51, CYP52 and CYP61. It also encodes one NADPH-P450 reductase (NPR) that can deliver electrons to both P450 enzymes and heme oxygenase (http://www.candidagenome.org/) [4].

Candida albicans is a well known pathogenic fungus of opportunistic oral and vaginal infections in humans [5,6]. Due to the recent increase in immunocompromised patients caused by HIV, cancer chemotherapy, and organ/bone marrow transplantation, systemic infections of *C. albicans* remain a serious clinical problem [7,8]. A frequent occurrence of numeric and structural chromosomal shuffling in the *C. albicans* genome and the ability to switch its colony phenotype are its best-known adaptation characteristics [9].

The CYP51 family is very special, as there is a strict functional conservation of enzyme activity among its members in all biological kingdoms except for some nematodes and insects that lack CYP51 and therefore obtain sterols from their diet [10,11]. They all catalyze the same three sequential oxidative steps that remove the 14α-methyl group from post-squalene sterol precursors [10]. Azole antifungal agents are widely used in the treatment of fungal infections and fungal CYP51 enzymes are considered as their primary target [12]. However, the mechanism of antifungal action at the molecular level has not yet been fully clarified. Azole inhibition of CYP51 in fungi causes accumulation of membrane-disrupting methylated ergosterol precursors that prevent fungal growth [13]. Azole drugs bind as a sixth ligand to the heme iron atom of CYP51 to give a Type II spectrum with a maximum at 430 nm and a minimum at 410 nm [14]. This interaction involves coordination of the iron with N3 of an imidazole ring or N4 of a triazole ring in the azoles.

* Corresponding author. Address: Department of Biological Sciences, Konkuk University, 1 Hwayang-dong, Gwangjin-gu, Seoul 143-701, South Korea. Fax: +82 2 3436 5432.
E-mail address: donghak@konkuk.ac.kr (D. Kim).

[1] *Abbreviations used:* P450 (or CYP), cytochrome P450; PCR, polymerase chain reaction; TB, terrific broth; DTT, dithiothreitol; NPR, NADPH-P450 reductase; CHAPS, 3-[(3-cholamidopropyl)dimethylammonio]-1-propanesulfonate.

0003-9861/$ - see front matter © 2011 Elsevier Inc. All rights reserved.
doi:10.1016/j.abb.2011.02.002

Azole-resistant strains have emerged as a serious problem in the clinical use of azole drugs in the treatment to *C. albicans* infections. Amino acid substitutions in CYP51F1 gene sequences have been found in azole-resistant *C. albicans* isolates [14,15]. Interestingly, in the studies of isolates from patients during the emergence of resistance, increased transcriptional levels of CYP51F1 and the drug transporters CDR and MDR1 were observed in addition to the mutations in the CYP51F1 amino acid sequence [16,17]. Variations in the *CYP51F1* gene are thought to be associated with resistance to azole antifungal agents, but few detailed biochemical studies at the protein level have so far addressed this problem.

In this study, we have successfully cloned, overexpressed, and purified CYP51F1 and several of its variants from *C. albicans* and characterized these proteins in terms of their spectroscopic and catalytic properties.

Materials and methods

Chemicals and enzymes

Lanosterol, econazole, fluconazole, itraconazole, ketoconazole, sodium dithionite, glucose-6-phosphate, glucose-6-phosphate dehydrogenase, and $NADP^+$ were purchased from Sigma (St. Louis, MO) or Aldrich Chemical Co. (Milwaukee, WI). Other chemicals were of the highest grade commercially available. *Escherichia coli* DH5α cells were purchased from Invitrogen (Carlsbad, CA). Recombinant rat NPR was expressed in *E. coli* and purified as previously reported [18].

Construction of expression plasmids and site-directed mutagenesis

The general approach has been described previously [19,20]. The genomic DNA from *C. albicans* was kindly provided by Professor Won Ki Huh at Seoul National University. The open reading frame for CYP51F1, and an added 6xHis-C-terminal tag, were amplified using PCR with forward and reverse primers (5′-AAACA GGATCCATCGATGCTTAGGAGGTCATATGGCTATTGTTGAAAC-′3, 5′-ATTATTTCTAGACCGGAAGCTTTTAGTGATGGTGATGGTGATGAAACA TACAAGTTTCTCT-′3) and the amplified PCR fragment was cloned into the pCW(Ori^+) vector using the *BamH*I and *Xba*I restriction sites. The cloned vectors were verified by nucleotide sequencing analysis and restriction digestion. *C. albicans* translates CTG as Ser instead of Leu, the amino acid for which CTG is a universal codon [21]. The open reading frame of CYP51F1 contains a CTG encoding a Ser that must be corrected by site-directed mutagenesis to enable expression of the correct recombinant protein in *E. coli*. Site-directed mutagenesis to change Leu263 to a Ser was carried out using Quick-Change mutagenesis (Stratagene, La Jolla, CA) as previously described [20]. Four CYP51F1 variant clones containing F105L, Y132H, D116E, and R467K substitutions were constructed by site-directed mutagenesis.

Enzyme expression and purification

Expression and purification of the CYP51F1 enzyme were carried out as previously described with some modifications [22]. Briefly, the *E. coli* strains transformed with pCW(Ori^+) vectors were inoculated into TB medium containing 100 μg/ml ampicillin and 1.0 mM IPTG. The expression cultures were grown at 37 °C for 3 h and then at 28 °C with shaking at 200 rpm for 24 h in 1 l Fernbach flasks. Bacterial inner membrane fractions containing CYP51F1 were isolated and prepared from 1 l TB (with ampicillin, 100 μg/ml) expression cultures of *E. coli* DH5α. Purification of CYP51F1 enzyme using a Ni^{2+}-nitrilotriacetate column was as previously described [22,23]. Briefly, membranes were solubilized at 4 °C overnight in 100 mM potassium phosphate buffer (pH 7.4) containing 20% (w/v) glycerol, 0.5 M NaCl, 10 mM β-mercaptoethanol, and 1.5% (w/v) CHAPS. The solubilized fraction was then loaded onto a Ni^{2+}-nitrilotriacetate column (Qiagen, Valencia, CA) and the purified protein was obtained with the elution buffer con-

```
CaCYP51     MAIVETVID- GI-------- ---------- NYFLSLSVTQ QISILLGVPF VYNLVWQYLY SL---RKDRA PLVFYWIPWF GSAASYGQQP YEFFESCRQ-
HsCYP51     MAAAAGMLLL GLLQAGGSVL GQAMEKVTGG NLL-SM-LLI ACAFTLSLVY LIRLAAGHLV QLPA-GVKSP PYIFSPIPFL GHAIAFGKSP IEFLENAYE-
MtCYP51     MSAVAL---- ---------- ---------- ---------- ---------- ---------- ---------- PRVSGGHDEH GHLEEFRTDP IGLMQRVRD-
TcCYP51     MFIEAIV--- ---------- ---------- ---------- -----LALTA LILYSVYSVK SFNTTRPTDP PVYPVTVPFL GHIVQFGKNP LEFMQRCKRD

                                   *                    *                    *
CaCYP51     KYGDVFSFML LGKIMTVYLG PKGHEFVFNA KLSDVSAEDA YKHLTTPVFG KGVIYDCPNS RLMEQKKFAK FALTTDSFKR YVPKIREEIL NYFVTDESFK
HsCYP51     KYGPVFSFTM VGKTFTYLLG SDAAALLFNS KNEDLNAEDV YSRLTTPVFG KGVAYDVPNP VFLEQKKMLK SGLNIAHFKQ HVSIIEKETK EYFES---W-
MtCYP51     ECGDVGTFQL AGKQVVLLSG SHANEFFFRA GDDDLDQAKA YPF-MTPIFG EGVVFDASPE RRKEMLH--N AALRGEQMKG HAATIEDQVR RMIAD---W-
TcCYP51     LKSGVFTISI GGQRVTIVGD PHEHSRFFSP RNEILSPREV YTI-MTPVFG EGVAYAAPYP RMREQLNFLA EELTIAKFQN FVPAIQHEVR KFMAEN--W-

CaCYP51     LKEKT-HGVA NVMKTQPEIT IFTASRSLFG DEMRRIFDR- SFAQLYSDLD KGFTPINFVF P---NLPLPH YWRRDAAQKK ISATYMKEIK SRRER-GDID
HsCYP51     ---GE-SGEK NVFEALSELI ILTASHCLHG KEIRSQLNE- KVAQLYADLD GGFSHAAWLL PG--WLPLPS FRRRDRAHRE IKDIFYKAIQ KRRQS-Q---
MtCYP51     ---GE-AGEI DLLDFFAELT IYTSSACLIG KKFRDQLDG- RFAKLYHELE RGTDPLAYVD P---YLPIES FRRRDEARNG LVALVADIMN GRIAN-PPTD
TcCYP51     ---KEDEGVI NLLEDCGAMI INTACQCLFG EDLRKRLNAR HFAQLLSKME SSLIPAAVFM PWLLRLPLPQ SARCREARAE LQKILGEIIV AREKEEASKD

CaCYP51     -PNRDLIDSL LIHSTYKDGV -KMTDQEIAN LLIGILMGGQ HTSASTSAWF LLHLGEKPHL --QDVIYQEV VELLKEKGGD -LNDLTYED- LQKLPSVNNT
HsCYP51     EKIDDILQTL -LDATYKDGR -PLTDDEVAG MLIGLLLAGQ HTSSTTSAWM GFFLARDKTL --QKKCYLE- ---QKTVCGE NLPPLTYDQ- LKDLNLLDRC
MtCYP51     KSDRDMLDVL -IAVKAETGT PRFSADEITG MFISMMFAGH HTSSGTASWT LIELMRHRDA --YAAVIDE- ---LDELYGD -GRSVSFHA- LRQIPQLENV
TcCYP51     NNTSDLLGGL -LKAVYRDGT -RMSLHEVCG MIVAAMFAGQ HTSTITTSWS MLHLMHPKNK KWLDKLHKE- ---IDEFP-- --AQLNYDNV MDEMPFAERC

CaCYP51     IKETLRMHMP LHSIFRKVTN PLRIPETNYI VPKGHYVLVS PGYAHTSERY FDNPEDFDPT RWDTAAAKAN SVSFNSSDEV DYGFGKVSKG VSSPYLPFGG
HsCYP51     IKETLRLRPP IMIMMRMART PQTV--AGYT IPPGHQVCVS PTVNQRLKDS WVERLDFNPD RYLQDNPAS- ---------- --------G- EKFAYVPFGA
MtCYP51     LKETLRLHPP LIILMRVAKG EFEV--QGHR IHEGDLVAAS PAISNRIPED FPDPHDFVPA RYEQPRQED- ---------- --------LL NRWTWIPFGA
TcCYP51     VRESIRRDPP LLMVMRMVKA EVKV--GSYV VPKGDIIACS PLLSHHDEEA FPNPRLWDPE RDEKV----- ---------- ---------- -DGAFIGFGA

                *
CaCYP51     GRHRCIGEQF AYVQLGTILT TFVYNLRWTI DGYKV-PDPD YSSMVVLPTE PAE-IIWEKR ETCMF
HsCYP51     GRHRCIGENF AYVQIKTIWS TMLRLYEFDL IDGYF-PTVN YTTMIHTPEN P-V-IRYKRR S---K
MtCYP51     GRHRCVGAAF AIMQIKAIFS VLLREYEFEM AQPPESYRND HSKMVVQLAQ PAC-VRYRRR TG--V
TcCYP51     GVHKCIGQKF ALLQVKTILA TAFREYDFQL LRDEV-PDPD YHTMVVGPTL NQCLVKYTRK KKLPS
```

Fig. 1. Sequence alignment of *C. albicans* CYP51F1 with other CYP51 enzymes. The amino acid sequences were aligned using the software T-Coffee (http://www.tcoffee.org). The residues corresponding to the conserved heme binding sites in the CYP51 family are shown with boxes. The alignment scores of *C. albicans* CYP51F1 to human, *Mycobacterium tuberculosis*, and *Trypanosoma cruzi* CYP51's were 86, 87, and 85, respectively.

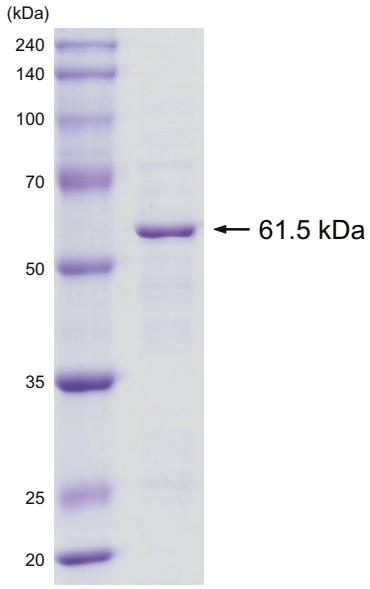

Fig. 2. SDS–PAGE of the purified CYP51F1 protein.

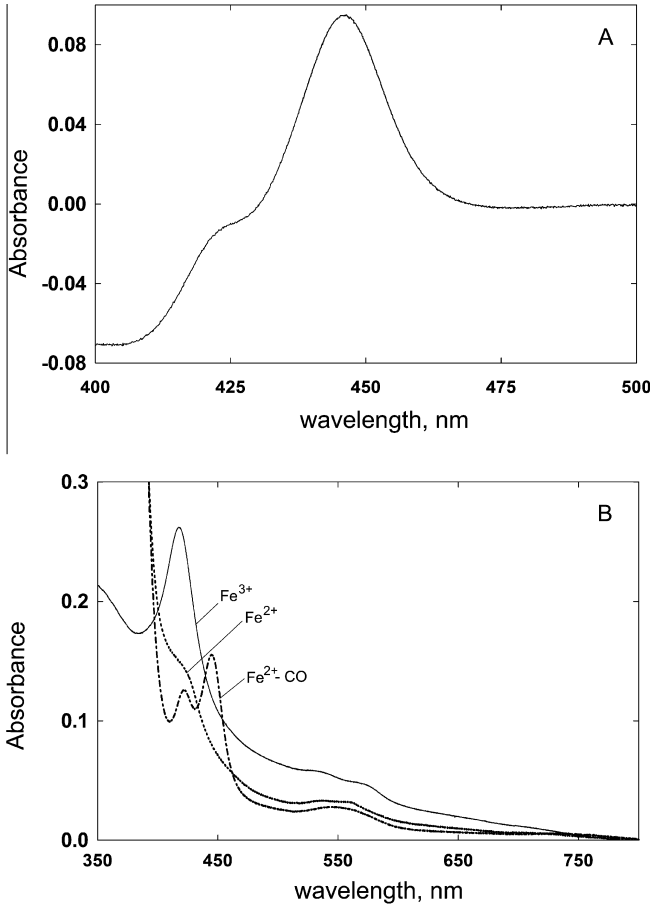

Fig. 3. Spectral analysis of the purified CYP51F1 protein. (A) The Fe^{2+}·CO vs Fe^{2+} difference spectrum and (B) the absolute spectra of the Fe^{3+}, Fe^{2+}, and Fe^{2+}·CO forms were recorded.

taining 400 mM imidazole. Eluted fraction containing P450 was dialyzed at 4 °C against 100 mM potassium phosphate buffer (pH 7.4) containing 20% (v/v) glycerol, 0.1 mM EDTA.

Spectroscopic characterization

The CO-P450 complexes were generated by passing CO gas through solutions of the P450. Then, sodium dithionite was added to reduce the purified ferric CYP51F1 enzymes. UV–visible spectra were collected on a CARY 100 Varian spectrophotometer in 100 mM potassium phosphate buffer (pH 7.4) at room temperature.

Spectral binding titrations

Purified CYP51F1 wild-type and variant enzymes were diluted to 2 μM in 100 mM potassium phosphate buffer (pH 7.4) and divided between two glass cuvettes. Spectra (350–500 nm) were recorded with subsequent additions of substrate (lanosterol) or azole compounds (in methanol stock) using a CARY 100 Varian spectrophotometer [24]. The difference in absorbance between the wavelength maximum and minimum was plotted versus the substrate concentration [25,26]. The data were fit to the typical hyperbolic equation for lanosterol and the quadratic equation for azole drugs using nonlinear regression analysis with Graph-Pad Prism software (Graph-Pad, San Diego, CA).

Lanosterol demethylation assay

Lanosterol demethylation by CYP51F1 was determined using a P450/NPR/phospholipid reconstituted system. The reaction mixture included 100 pmol purified P450 enzyme, 200 pmol rat NPR, and DLPC (45 μM) in 0.50 ml of 100 mM potassium phosphate buffer (pH 7.4), along with lanosterol (200 μM). An NADPH-generating system [26] was used to start reactions. Incubations were generally done for 30 min at 37 °C and terminated by addition of l ml of CH_2Cl_2. The CH_2C_2 extract was dried under N_2 and then converted to trimethylsilyl derivatives by incubation with 50 μl of *N,O*-bis(trimethylsilyl)trifluoroacetamide at 70 °C for 10–15 min. The derivatized samples were allowed to cool, vortexed, and transferred to sealed Teflon-capped glass vials for either manual or autoinjection into the GC-MS. Analyses were performed on an Agilent 6850 gas chromatograph coupled to an Agilent 5973 Network Mass Selective Detector using electron ionization (EI) as previously described [27].

Homology modeling

A molecular model of *C. albicans* CYP51F1 structure was constructed using the X-ray crystal structure of *Mycobacterium tuberculosis* CYP51 (PDB 1EA1) as a template. The coordinates of the model were obtained using the SWISS-MODEL software from the Swiss Institute of Bioinformatics (http://www.swissmodel.expasy.org/).

Results

Sequence alignment with other P450s

The *ERG11* gene from *C. albicans* (Genebank: X13296, orf19_922)[2] encodes CYP51F1 (lanosterol 14α-demethylase), a member of the cytochrome P450 family that functions in ergosterol biosynthesis. Phylogenetically, CYP51 enzymes are highly conserved throughout nature from bacteria, through fungi, to humans. Amino acid sequence alignment of CYP51F1 from *C. albicans* with CYP51

[2] CYP51F1 from *C. albicans* is the ERG11 gene (Genebank: X13296, orf19_922) encoding lanosterol 14α-demethylase and it has an amino acid sequence similarity score of 86% with that of human CYP51A1 (NM_000786) lanosterol 14?-demethylase (http://drnelson.uthsc.edu/cytochromeP450.html).

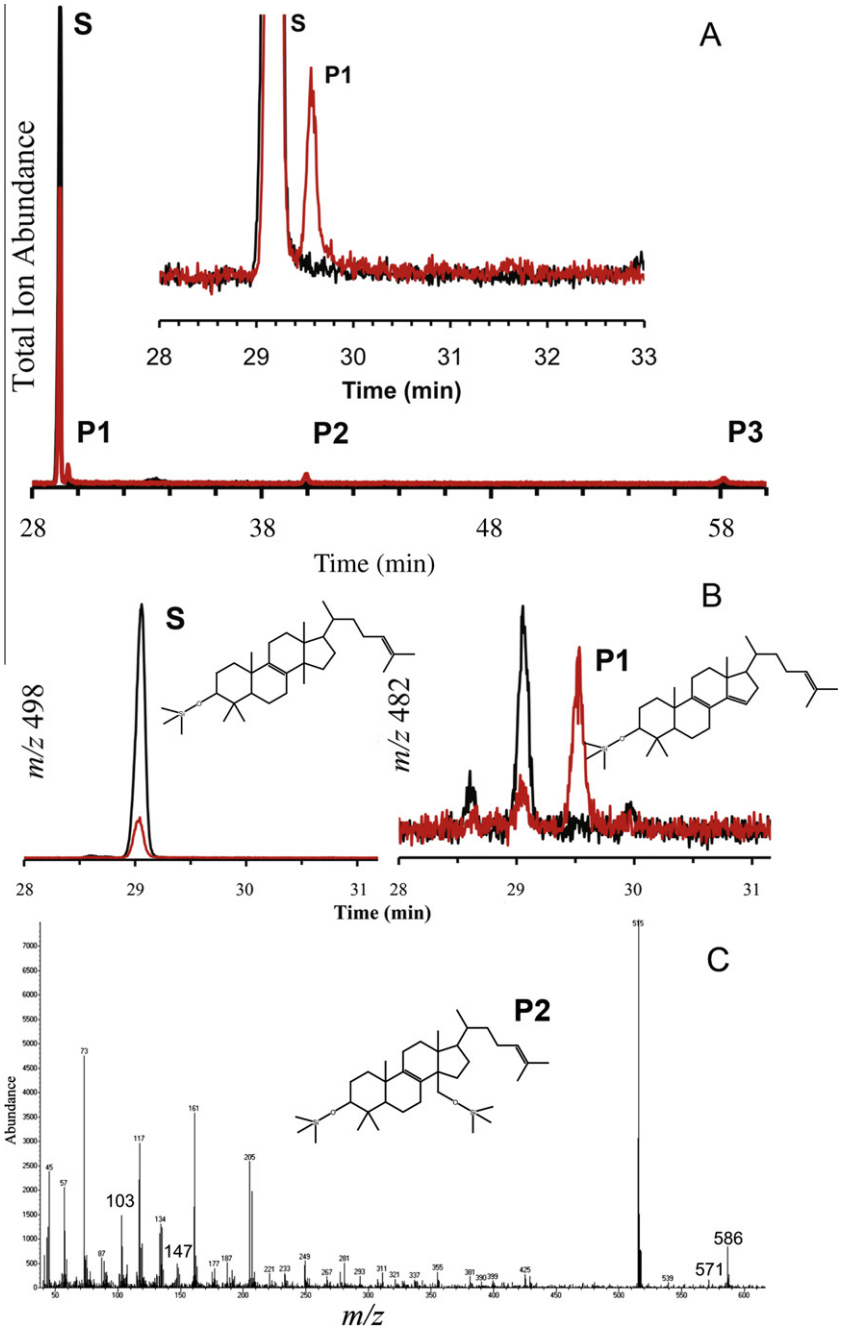

Fig. 4. GC–MS of products formed in the reaction of CYP51F1 with lanosterol. (A) GC–MS total ion trace of the reaction products, with the inset showing an expanded view of the substrate (lanosterol) and FF-MAS (P1); (B) CYP51F1 reactions and controls were also analyzed in selected ion monitoring (SIM) mode. The SIM spectra for *m/z* 498 and *m/z* 482 correspond to lanosterol and FF-MAS, respectively. For each SIM spectrum the RED trace corresponds to CYP51F1 incubations while the black spectrum represents control reactions. (C) Elecron impact mass-spectrum of hydroxylanosterol TMS-ether (P2). The molecular ion $[M]^{+\bullet}$ is found at *m/z* 586, M – CH_3 at *m/z* 571, and the signature ion at *m/z* 103 corresponds to loss of CH_2OTMS from a primary alcohol.

of other species reveals high sequence similarities with scores from 85% to 87% identity (Fig. 1) [28]. Good sequence alignment with human, *M. tuberculosis*, and *Trypanosoma cruzi* CYP51 suggests that the gene product *ERG11* from *C. albicans* is likely to have lanosterol 14α-demethylase catalytic activity.

Expression and purification of CYP51F1

The reduced CO-binding spectrum in the whole cell culture showed the typical P450 expression level of ~50 nmol P450 holoenzyme per liter of culture medium (data not shown). After ultracentrifugation, the expressed P450 protein was observed in the membrane fraction. CHAPS successfully solubilized the membrane-bound P450 protein and the solubilized protein was purified on a Ni-column. The resulting protein migrated on SDS–PAGE as a single band at 61.5 kDa, as expected for the open reading frame of the CYP51F1 gene with a His-tag (Fig. 2). Protein sequencing of the purified protein by mass-spectrometry indicated that the purified protein was the expected CYP51F1 from *C. albicans* (Supplementary Fig. 1).

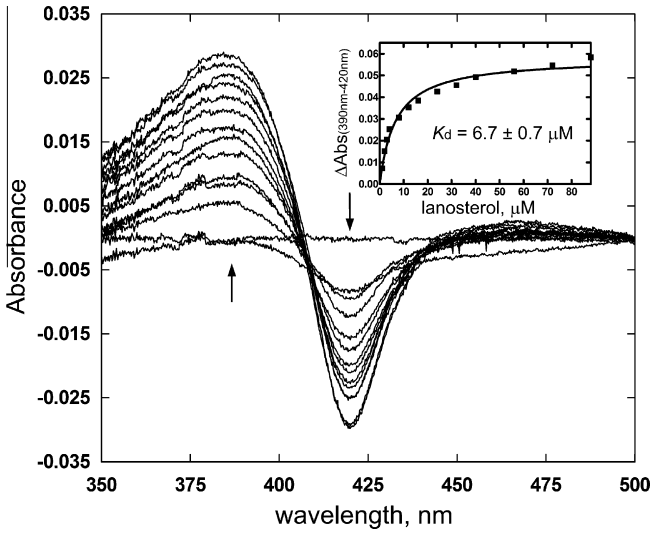

Fig. 5. Titration of CYP51F1 with lanosterol. Increasing concentrations of lanosterol were added to both the sample and reference cuvettes. The inset shows the plot of $\Delta A_{390-420\ nm}$ vs. concentration of lanosterol.

Spectral properties of CYP51F1

The reduced CO-difference spectrum of purified CYP51F1 had a maximum absorption at 446 nm (Fig. 3A). Examination of the absolute spectrum showed that the ferric form of the protein was in the low spin state with a Soret band at 419 nm, while the ferrous protein had a broad absorption peak around 420 nm (Fig. 3B). The smaller α-, and β-bands of the ferric P450 were at 568 and 536 nm, respectively (Fig. 3B). On reduction with sodium dithionite, the α-, and β-bands shifted to 559 and 530 nm respectively.

Catalytic activities of CYP51F1

Purified CYP51F1 reconstituted with rat NPR supported the catalytic turnover of lanosterol to yield three GC–MS detectable products (Fig. 4A). The first product peak (P1) in the chromatogram was determined as the final 14α demethylated metabolite (FF-MAS, follicular fluid-meiosis activating steroid) of lanosterol, although it was partially masked by the tail of the lanosterol peak. Selected ion monitoring (SIM) scans for $m/z = 498$ (lanosterol TMS ether) and also $m/z = 482$ (FF-MAS TMS ether) confirmed that peak P1 did in fact correspond to FF-MAS (Fig. 4B). The second product peak (P2) was consistent with the product of oxidation of the methyl to

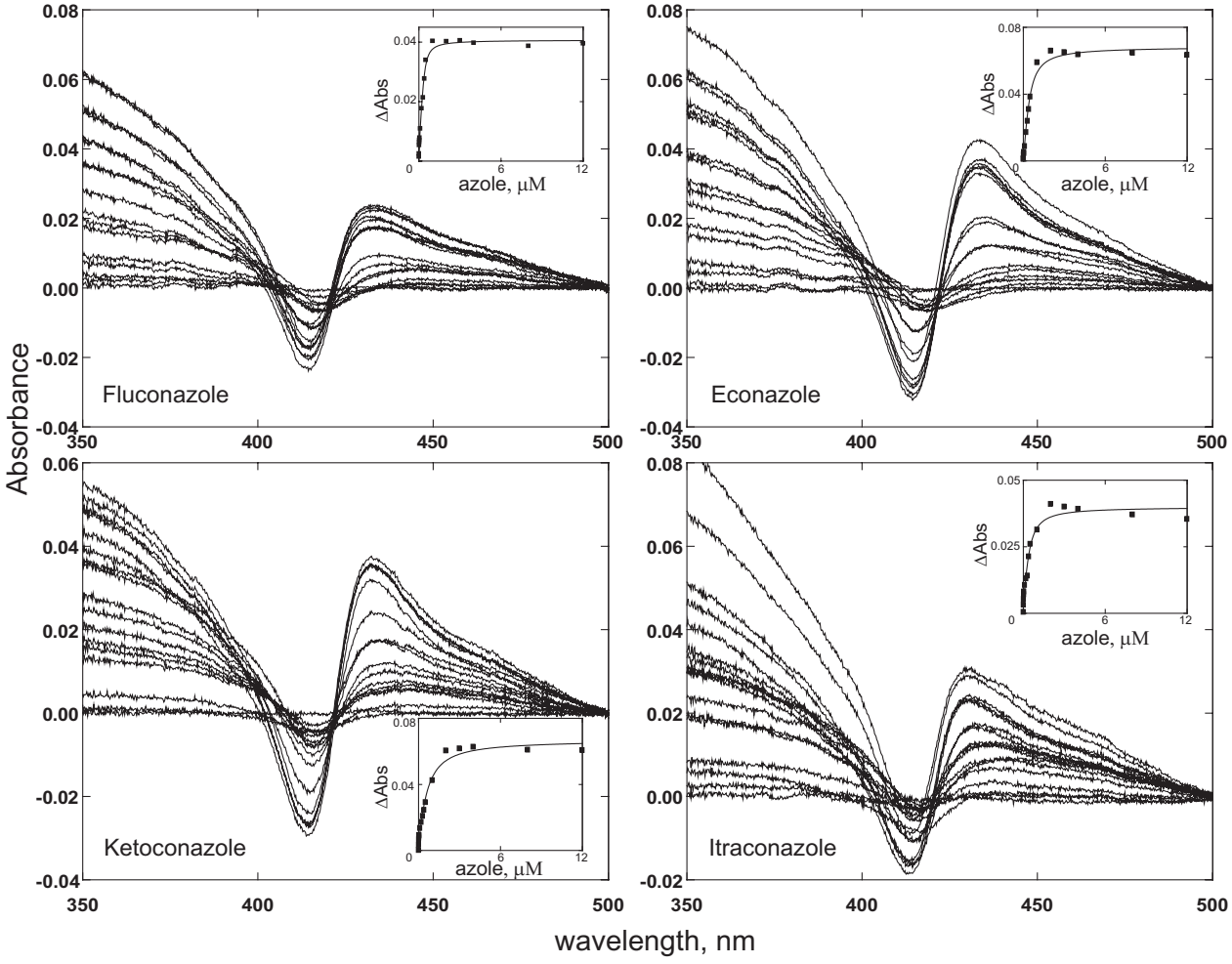

Fig. 6. Titration of CYP51F1 with azole compounds. Purified CYP51F1 (2 μM) was dissolved in 100 mM potassium phosphate buffer (pH 7.4) and the absorption spectrum of the ferric form (350–500 nm) was recorded with subsequent additions of the azole compound fluconazole, econazole, ketoconazole, or itraconazole. The binding affinities of the azoles calculated from the plots are shown in Table 1.

Table 1
Binding affinities of azole agents to the *C. albicans* CYP51F1 wild-type and mutant proteins.

Azole agents	K_d (μM)				
	Wild type	F105L	D116E	Y132H	R467 K
Econazole	0.20 ± 0.04	0.10 ± 0.03	0.14 ± 0.03	0.42 ± 0.06	0.13 ± 0.03
Fluconazole	0.06 ± 0.01	0.02 ± 0.01	0.03 ± 0.01	0.15 ± 0.06	0.06 ± 0.01
Itraconazole	0.19 ± 0.06	0.16 ± 0.04	0.15 ± 0.03	ND[a]	0.18 ± 0.04
Ketoconazole	0.42 ± 0.08	0.17 ± 0.04	0.43 ± 0.08	0.54 ± 0.07	0.66 ± 0.13

[a] Not determined.

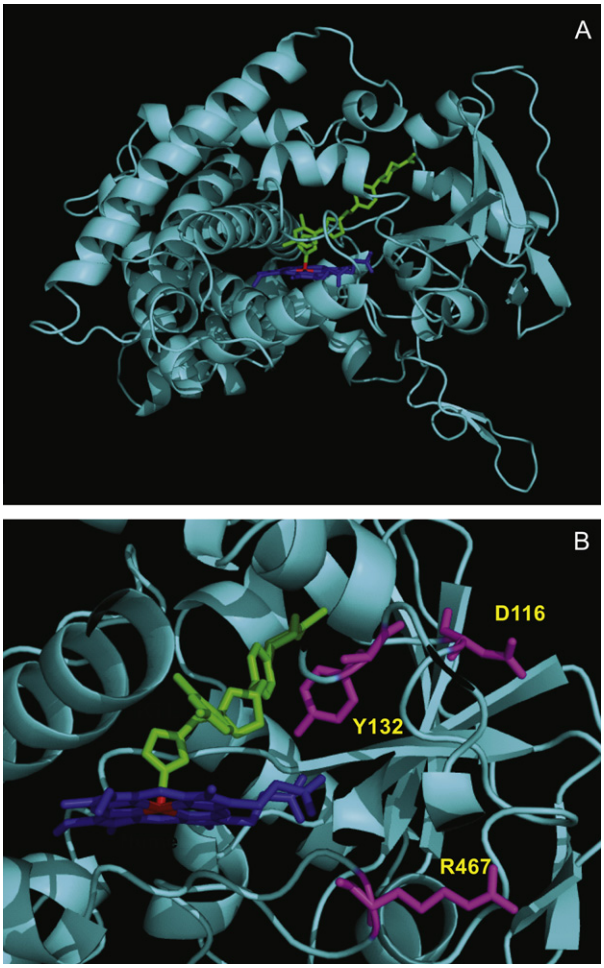

Fig. 7. Positions of the mutated amino acid residues in CYP51F1. (A) Ribbon diagram of the *C. albicans* CYP51F1 model using the X-ray crystal structure of *M. tuberculosis* CYP51 (PDB 1EA1) as a template and (B) the positions of the Y132, D116, and R476 mutations are indicated with colors. Heme and fluconazole are shown in blue and green, respectively.

the alcohol, the expected first step of lanosterol demethylation (Fig. 4C). Its fragmentation pattern was consistent with the TMS-ether. The third product (P3) could not be identified. It had a mass 44 Da higher than that of the alcohol but did not fit with any of the intermediates expected in the multi-step demethylation mechanism.

Binding of lanosterol and azole agents to CYP51F1 wild type and variants

Titration of purified CYP51F1 with lanosterol showed a typical type I spectral change with an increase at 390 nm and decrease at 420 nm, consistent with displacement of the iron-bound water molecule by the lanosterol to give a low-spin hexa coordinated P450 heme (Fig. 5). The calculated K_d value is 6.7 ± 0.7 μM (Fig. 5). Furthermore, purified CYP51F1 produced a typical type II spectral change, with an increase at 430 nm and a decrease at 410 nm, on binding of azole drugs (Fig. 6), as expected for the binding of a strong ligand to the heme iron atom [29]. The calculated K_d values for the azole drugs are between 0.06 and 0.42 μM (Table 1).

Mutations that occur frequently in the CYP51F1 gene (F105L, D116E, Y132H, and R467K) in clinically isolated azole-resistant *C. albicans* strains were analyzed to determine their effect on the binding affinity of azole drugs [15]. Recombinant mutant enzymes were expressed and purified as already described. There were no notable differences in the reduced-CO difference and absolute spectra (data not shown). Three of the mutant proteins bound azole agents to give typical type II spectra (Supplementary Figs. 2–5). However, binding of azoles to the Y132H mutant showed the expected decrease at 410 nm but little increase at 430 nm (Supplementary Fig. 4). Unexpectedly, the K_d values for the binding of azoles to the purified F105L, D116E, and R467K mutants were little altered (Table 1). The binding of lanosterol to the purified F105L, D116E, and R467K mutants occurred with a type I spectral change and binding affinities similar to those for the wild-type enzyme (Supplementary Fig. 6). Titration of the Y132H mutant with lanosterol gave the expected decrease at 425 nm, but the distinct increase in the peak at 390 nm was not observed.

Discussion

We previously reported purification and characterization of CYP52A1, the *Alk8* gene product from *C. albicans* [30], that oxidizes dodecanoic acid to the ω-hydroxylated metabolite as a major product and the (ω-1)-hydroxylated compound as a minor one. A functional heme oxygenase from *C. albicans*, the product of the *CaHmx1* gene, has also been characterized [20]. Recently, the NPR of *C. albicans*, coded by the *NCP1* gene, was characterized [31]. The purified *C. albicans* NPR was shown to be an orthologous reductase that supports both the cytochrome P450 and heme oxygenase activities. Our present biochemical characterization of CYP51F1 from *C. albicans* complements these earlier studies and broadens our understanding of the critical system of catalytic hemoproteins in *C. albicans*.

The *ERG11* gene in *C. albicans* encodes CYP51F1, a putative sterol 14α-demethylase, that is required for the biosynthesis of ergosterol. Indeed, purified CYP51F1 converts lanosterol to its demethylated product through initial formation of the alcohol metabolite, but the conversion rate is relatively low (Fig. 4). The aldehyde intermediate expected in the oxidation sequence was not detected, possibly because it is too rapidly oxidized to the acid intermediate. One caveat in the assignment of oxidized products is that the identification of the site of hydroxylation is still putative since it was based only on mass spectral evidence. However, the mass spectrometric evidence is commonly used for these types of metabolites when the metabolite standards are not available [27,32,33]. HPLC analysis of the enzyme reactions were performed to obtain the enzyme oxidation

rate. A new peak appeared in the chromatogram, assuming the putative lanosterol oxidation product (Supplementary Fig. 8A). But, the identification of the product mass was failed due to no ionization in LC-mass spectrometry. The rate of oxidation of lanosterol based on this HPLC analysis was estimated with assuming the new peak as the lanosterol oxidation product. The calculated k_{cat} value was approximately 0.19 min^{-1} with a K_m value of 20 μM for the wild-type CYP51F1 enzyme (Supplementary Fig. 8B). In addition, the putative oxidation product peak disappeared when the lanosterol oxidation reaction was performed with azole compounds, suggesting that the oxidation activity of purified enzyme was inhibited by azole drugs (Supplementary Fig. 8A).

Site-specific mutations in the CYP51F1 gene have been considered as one of the main mechanisms for azole resistance in clinically isolated *C. albicans* strains. So far, about 140 mutations have been reported in the literature, but few of them have been specifically associated with azole resistance [34]. Multiple mechanisms of resistance have been proposed, including a reduction of intracellular azole concentration or an increased CYP51 expression [14]. Changes in CYP51F1 expression have been detected in resistant strains, but their role in resistance is unclear.

Based on a homology model of *C. albicans* CYP51F1, we postulate that Tyr132 in the BC loop is located close to the heme in the active site (Fig. 7) and mutations of this residue are likely to modify the active site architecture and heme environment. Kudo et al. [35] reported that an Y132H substitution modified the heme environment but fluconazole resistance was predominantly associated with the double Y132H/F145L mutations. Unusual spectra were obtained on binding of lanosterol or azole drugs to the Y132H mutant in this study. This observation suggests that modification of the heme environment by the substitution Y132H may be a prerequisite for the effective resistance to azole drugs conferred by multiple mutations.

Interestingly, our study indicated that the azole resistance observed in clinical isolates of *C. albicans* does not necessarily result only from a lowering of the azole binding affinity of CYP51F1. Thus, at least the four purified mutant enzymes in this study did not show a direct correlation between azole affinity and resistance. Recently, Warrilow et al. [36] also reported that the azole resistance conferred by a I471T mutation of CYP51F1 is not due to significantly alteration of the enzyme's affinity for azole compounds. They postulated that the increased resistance to azoles conferred by the I471T substitution reflected an enhanced ability of the I471T mutant to remain functionally active at high azole concentrations [36]. Therefore, the mutant enzymes may acquire azole resistance through a combination of mechanisms, not simply by a decreased azole binding affinity. However, *C. albicans* mutant CYP51F1 enzymes may produce enough ergosterol to maintain cell viability, even if at a very low rate of turnover, despite the presence of a high azole concentration. Measurements of the amount of lanosterol produced by purified mutant enzymes in the presence of high concentrations of azole drugs may provide a clue relative to this postulated mechanism of azole resistance and is currently under investigation.

In conclusion, we have overexpressed, purified, and characterized a critical P450 enzyme from the pathogenic fungus *C. albicans*. The purified CYP51F1 catalyzes lanosterol demethylation and, interestingly, four of its mutants from azole-resistant strains retain essentially unchanged binding affinities for azole drugs. Structure–function studies of this *C. albicans* CYP51F1 enzyme will provide the basis for the improved design of azole drugs against this pathogen.

Acknowledgments

This study was supported by a grant to D.K. from the Korea Healthcare Technology R&D Project, Ministry for Health, Welfare & Family Affairs, Republic of Korea (A084005), and by National Institutes of Health Grant GM25515 to P.R.O.M.

Appendix A. Supplementary data

Supplementary data associated with this article can be found, in the online version, at doi:10.1016/j.abb.2011.02.002.

References

[1] F.P. Guengerich, Z. Tang, S.G. Salamanca-Pinzon, Q. Cheng, Mol. Interv. 10 (2010) 153–163.
[2] P.R. Ortiz de Montellano, In: P.R. Ortiz de Montellano (Ed.), Cytochrome P450: Structure, Mechanism, and Biochemistry, Plenum Press, New York, 2005.
[3] D.R. Nelson, L. Koymans, T. Kamataki, J.J. Stegeman, R. Feyereisen, D.J. Waxman, M.R. Waterman, O. Gotoh, M.J. Coon, R.W. Estabrook, I.C. Gunsalus, D.W. Nebert, Pharmacogenetics 6 (1996) 1–42.
[4] C. dEnfert, S. Goyard, S. Rodriguez-Arnaveilhe, L. Frangeul, L. Jones, F. Tekaia, O. Bader, A. Albrecht, L. Castillo, A. Dominguez, J.F. Ernst, C. Fradin, C. Gaillardin, S. Garcia-Sanchez, P. de Groot, B. Hube, F.M. Klis, S. Krishnamurthy, D. Kunze, M.C. Lopez, A. Mavor, N. Martin, I. Moszer, D. Onesime, J. Perez Martin, R. Sentandreu, E. Valentin, A.J. Brown, Nucleic Acids Res. 33 (2005) D353–D357.
[5] F.C. Odds, Crit. Rev. Microbiol. 15 (1987) 1–5.
[6] M.L. Pendrak, M.P. Chao, S.S. Yan, D.D. Roberts, J. Biol. Chem. 279 (2004) 3426–3433.
[7] P.L. Fidel, Jr., 2002. Oral Dis. 8 (Suppl. 2), 69–75.
[8] B.J. Kullberg, A.M. Oude Lashof, Eur. J. Med. Res. 7 (2002) 183–191.
[9] R. Calderone, F.C. Odds, T. Boekhout, FEMS Yeast Res. 9 (2009) 971–972.
[10] G.I. Lepesheva, T.Y. Hargrove, Y. Kleshchenko, W.D. Nes, F. Villalta, M.R. Waterman, Lipids 43 (2008) 1117–1125.
[11] N. Strushkevich, S.A. Usanov, H.W. Park, J. Mol. Biol. 397 (2010) 1067–1078.
[12] Y. Koltin, C.A. Hitchcock, Curr. Opin. Chem. Biol. 1 (1997) 176–182.
[13] N.H. Georgopapadakou, T.J. Walsh, Antimicrob. Agents Chemother. 40 (1996) 279–291.
[14] S.L. Kelly, D.E. Kelly, C.J. Jackson, A.G.S. Warrilow, D.C. Lamb, In: P.R. Ortiz de Montellano (Ed.), Cytochrome P450: Structure, Mechanism, and Biochemistry, Plenum Press, New York, 2005, pp. 585–617.
[15] P. Marichal, L. Koymans, S. Willemsens, D. Bellens, P. Verhasselt, W. Luyten, M. Borgers, F.C. Ramaekers, F.C. Odds, Microbiology 145 (Pt 10) (1999) 2701–2713.
[16] D. Sanglard, F. Ischer, M. Monod, Microbiology 143 (Pt 2) (1997) 405–416.
[17] R. Franz, S.L. Kelly, D.C. Lamb, D.E. Kelly, M. Ruhnke, J. Morschhauser, Antimicrob. Agents Chemother. 42 (1998) 3065–3072.
[18] I.H. Hanna, J.F. Teiber, K.L. Kokones, P.F. Hollenberg, Arch. Biochem. Biophys. 350 (1998) 324–332.
[19] D. Kim, F.P. Guengerich, Biochemistry 43 (2004) 981–988.
[20] D. Kim, E.T. Yukl, P. Moenne-Loccoz, P.R. Ortiz De Montellano, Biochemistry 45 (2006) 14772–14780.
[21] T. Ohama, T. Suzuki, M. Mori, S. Osawa, T. Ueda, K. Watanabe, T. Nakase, Nucleic Acids Res. 21 (1993) 4039–4045.
[22] D. Kim, Z.L. Wu, F.P. Guengerich, J. Biol. Chem. 280 (2005) 40319–40327.
[23] C.-H. Yun, G.P. Miller, F.P. Guengerich, Biochemistry 39 (2000) 11319–11329.
[24] C.H. Yun, K.H. Kim, M.W. Calcutt, F.P. Guengerich, J. Biol. Chem. 280 (2005) 12279–12291.
[25] J.B. Schenkman, H. Remmer, R.W. Estabrook, Mol. Pharmacol. 3 (1967) 113–123.
[26] F.P. Guengerich, in: A.W. Hayes (Ed.), Principles and Methods of Toxicology, Taylor & Francis, Philadelphia, 2001, pp. 1625–1687.
[27] X. He, M.J. Cryle, J.J. De Voss, J. Biol. Chem. 280 (2005) 22697–22705.
[28] C. Notredame, D.G. Higgins, J. Heringa, J. Mol. Biol. 302 (2000) 205–217.
[29] M.A. Correia, P.R. Ortiz de Montellano, In: Ortiz de Montellano, P.R. (Ed.), Cytochrome P450: Structure, Mechanism, and Biochemistry, Plenum Press, New York, 2005, pp. 247–322.
[30] D. Kim, M.J. Cryle, J.J. De Voss, Arch. Biochem. Biophys. 464 (2007) 213–220.
[31] H.G. Park, Y.R. Lim, C.Y. Eun, S. Han, J.S. Han, K.S. Cho, Y.J. Chun, D. Kim, Biochem. Biophys. Res. Commun. 396 (2010) 534–538.
[32] E.R. Trösken, E. Straube, W.K. Lutz, W. Völkel, C. Patten, J. Am. Soc. Mass. Spectrom. 15 (2004) 1216–1221.
[33] J. Acimovic, A. Lövgren-Sandblom, K. Monostory, D. Rozman, M. Golicnik, D. Lutjohann, I. Björkhem, J. Chromatog. B 877 (2009) 2081–2086.
[34] F. Morio, C. Loge, B. Besse, C. Hennequin, P. Le, Pape, Diagn. Microbiol. Infect. Dis. 66 (2010) 373–384.
[35] M. Kudo, M. Ohi, Y. Aoyama, Y. Nitahara, S.K. Chung, Y. Yoshida, J. Biochem. 137 (2005) 625–632.
[36] A.G. Warrilow, C.M. Martel, J.E. Parker, N. Melo, D.C. Lamb, W.D. Nes, D.E. Kelly, S.L. Kelly, Antimicrob. Agents Chemother. 54 (2010) 4235–4245.